sciendo

Nova Biotechnol Chim (2018) 17(2): 150-159
DOI: 10.2478/nbec-2018-0016

Nova Biotechnologica *et* Chimica

Synthesis of ternary bioactive glass derived aerogel and xerogel: study of their structure and bioactivity

Dalila Ksouri[1], Hafit Khireddine[1], Ali Aksas[1], Tiago Valente[2], Fatima Bir[1], Nadir Slimani[2], Belén Cabal[3], Ramón Torrecillas[3] and José Domingos Santos[2]

[1]*Laboratoire de Génie de l'Environnement (LGE), Faculté de Technologie, Université de Bejaia, Bejaia, 06000, Algerie*

[2]*Department of Materials, Faculty of Engineering, University of Porto (FEUP), Portugal*

[3]*Nanomaterials and Nanotechnology Research Center (CINN), CSIC - University of Oviedo (UO), Avda de la Vega 4-6, El Entrego 33940, San Martín del Rey Aurelio, Spain*

Article info

Article history:
Received: 7th June 2018
Accepted: 12th November 2018

Keywords:
Aerogel
Bioactive glass
Bioactivity
Sol-gel
63S

Abstract

In this work ternary bioactive glasses with the molar composition 63 % SiO_2, 28 % CaO, and 9 % P_2O_5 have been prepared via sol-gel processing route leading to xerogel or aerogel glasses, depending on the drying conditions. Two types of drying methods were used: atmospheric pressure drying (evaporative), to produce xerogels, and supercritical fluids drying, to obtain aerogels. Both dried gels were subjected to heat-treatment at three different temperatures: 400, 600 and 800 ºC in order to the removal of synthesis byproducts and structural modifications. The resulting materials were characterized by X-ray diffraction (XRD), Fourier transforms infrared spectroscopy (FTIR), scanning electron microscopy (SEM), thermal gravimetric analysis (TGA) and differential thermal analysis (DTA), and by *in vitro* bioactivity tests in simulated body fluid. The influence of the drying and the sintering temperature of their structure, morphology, and bioactivity of the final products were evaluated. The results show a good bioactivity of xerogel and aerogel bioactive glass powders with the formation of an apatite layer after one day of immersion in SBF solution for aerogel bioactive glass powders and a particle size less than 10 nm. An apatite layer formed after 3 days in the case of xerogel bioactive glass powders and a particle size around 100 nm.

Introduction

The bioactive glasses constitute an important group of biomaterials that have wide application in medical and dental fields (Mehdipour *et al.* 2012; Al-Noaman *et al.* 2012). In fact, when bioactive glasses are in contact with body fluid or tissue, they generate a series of physical and chemical reactions leading to the formation of hydroxyapatite surface layer (Zhitomirsky *et al.* 2009; Bellucci *et al.* 2011). Certain compositions of bioactive glasses containing SiO_2-CaO-P_2O_5 can bond to both soft and hard tissue without any intervening fibrous layer.

The method of elaboration of the bioactive glasses is greatly influencing the results of the bioactivity and biocompatibility. Sol-gel technique is the most widely used for the synthesis of bioactive glasses (Li *et al.* 2013). The sol-gel process involves hydrolysis, polymerization, gelation, drying, and a dehydration process. Gels are usually classified as aerogels and xerogels. When the liquid from the gel is evaporated at room temperature, the solid gels left behind are called xerogels. Whereas, when

✉ *Corresponding author:* dalidakso@gmail.com

the liquid from the gel is extracted at the supercritical state of liquid, these materials are called aerogels. The removal of solvent above its critical point occurs with no capillary pressure because there are no liquid-vapor interfaces. Thus in the aerogel process, there is a greatly reduced driving force for shrinkage (Catauro *et al.* 2015). The conditions of drying the gel and sintering temperature in the sol-gel method are also an important factor affecting the structure, morphology, and bioactivity of the bioactive glasses. The bioactivity responses depend upon the physical and chemical characteristics of the materials and particularly upon its chemical composition, crystallinity, particle size, surface structure, microstructure and surface roughness (Deligianni *et al.* 2001; Valerio *et al.* 2004). There has been increased interest in fabricating sol-gel derived nanoscale bioactive glasses. Nanoscale particulate bioactive glasses have shown advantages over conventional (micrometer-sized) bioactive glasses due to their large surface area and enhanced solubility as well as reactivity coupled with the possibility to induce nanotopographic surface features in composite materials (Erol-Taygun 2013).

In this work, ternary bioactive glasses with the molar composition 63 % SiO_2, 28 % CaO, and 9 % P_2O_5, known as 63S bioactive glass, have been prepared via sol-gel processing route leading to xerogel or aerogel glasses, depending on the drying conditions. In the literature, there are many articles about 63S obtained by atmospheric pressure drying (Catauro *et al.* 2015), but none by supercritical drying, at least for the author's knowledge. This paper compares the structure, morphology and *in vitro* bioactivity of identical chemical composition bioactive glasses produced by the sol-gel process at the supercritical condition of ethanol (aerogel) and by the most used synthesis route to obtain bioactive glasses (xerogel). The influence of the calcination temperatures was also evaluated.

Experimental

Preparation of bioactive glass powders

The composition of studied bioactive glass belongs to the ternary system SiO_2-CaO-P_2O_5 with 63S composition: 63 SiO_2 28 CaO 9 P_2O_5 (mol %). Glass powders were synthesized through a sol-gel process. Xerogel bioactive glasses (labelled as XG) were prepared in a similar way as previously described by other authors (Doostmohamadi *et al.* 2011). Briefly, tetraethylorthosilicate (TEOS), which was selected as a silica precursor for the sol, was added to ethanol as an alcoholic media and the mixture was stirred for 30 min. Distilled water was added to the solution and allowed to mix until the solution became clear with H_2O : TEOS molar ratio of 4 : 1. After 30 min, triethyl phosphate (TEP) was added to the stirring solution and after another 20 min, calcium nitrate tetrahydrate was added to the mixture. Hydrochloric acid (HCl, 2N) was used as a catalyst and the final solution was stirred for one hour additional. To obtain a xerogel bioactive glass powder (XG), the solution was heated at 60 °C for 10 h and dried at 130 °C for 20 h. Another identical solution was autoclaved at supercritical conditions of ethanol solvent (pressure of 63 bars, a temperature of 243 °C) to obtain an aerogel bioactive glass (labelled as AG).

The dried gel powders (xerogel and aerogel) were crushed and calcined at different temperatures: 400, 600 and 800 ºC, for 2 h with a heating rate of 5 °C/min, then the furnace was naturally cooled down. The obtained glasses were labelled as XG 400 and AG 400 when the calcination takes place at 400 °C, XG 600 and AG 600 when it was at 600 °C, XG 800 and AG 800 at 800 °C.

Characterization of bioactive glasses

Thermal behaviour of these bioactive glasses was performed with a thermogravimetric-differential thermal analyzer (TA Instruments, Q600) in a flowing air atmosphere at a heating rate of 5 ºC/min from the ambient temperature to 1,000 °C. X-ray diffraction (XRD) analysis of the bioactive glasses was conducted on a Bruker D8 Discover diffractometer using CuK α radiation (λ = 1,54060 Å) working at 40 kV and 40 mA in a step-scanning mode from 10° to 80°, at a scan speed of 0.04 °/s. The morphology of the obtained bioactive glasses was studied by scanning electron microscopy (SEM) Nova Nano SEM 200 equipped with the Silicon SUTW-Sapphire EDAX detector,

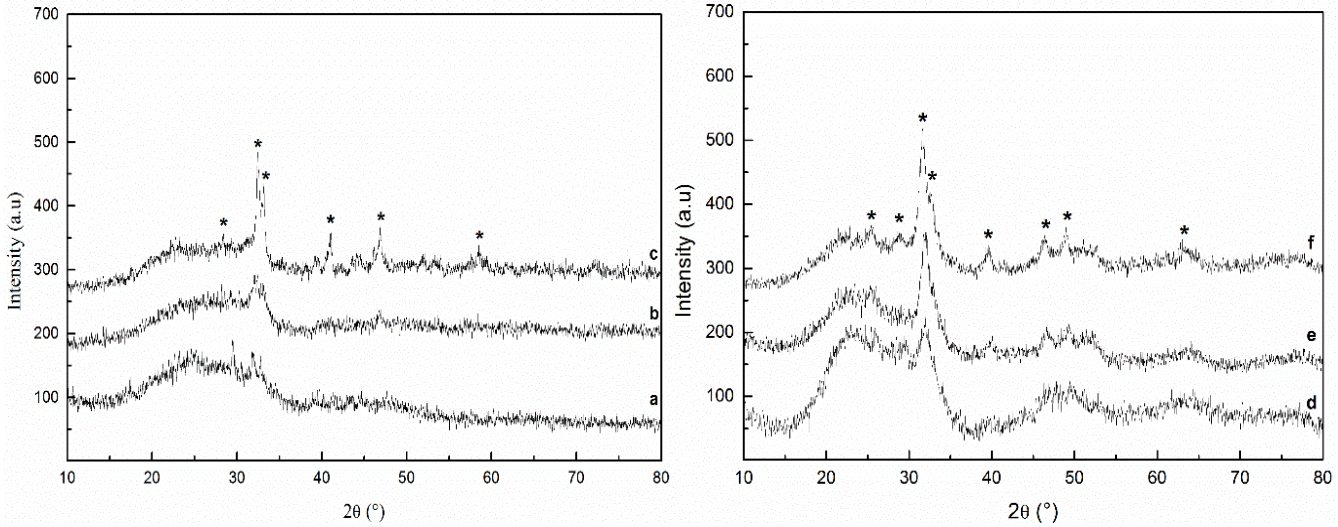

Fig. 1. XRD pattern of bioactive glass powders: a– XG 400, b– XG 600, c– XG 800, d– AG 400, e– AG 600 and f– AG 800.

resolution: 125.01. The microstructure of the surface of the samples *in vitro* tests was performed using a High resolution (Schottky) Environmental Scanning Electron Microscope with X-Ray Microanalysis and Electron Backscattered Diffraction analysis: Quanta 400 FEG ESEM / EDAX Genesis X4M. Samples were coated with Au/Pd thin film, by sputtering, using the SPI Module Sputter Coater equipment. Glasses were also characterized using transmission electron microscopy (TEM) (JEOL-2000EX).

In vitro bioactivity

The evaluation of *in vitro* bioactivity of the bioactive glass powders prepared by xerogel and aerogel at different calcined temperature was performed using SBF solution prepared according to Kokubo protocol (Kokubo 1990). *In vitro* bioactivity tests were used to evaluate the formation of an apatite layer on the surface of the bioactive glass pellets, considered as an indicator of *in vivo* bioactivity (Leonor *et al.* 2002). To study the bioactivity, the bioactive glass powders were pressed into pellets of 15 mm in diameter and 2 mm in thickness and were soaked in simulated body fluid (SBF) solution prepared according to the protocol developed by Kokubo (1990) at 37 °C and pH = 7.4 for 1, 3 and 7 days with a surface area to volume ratio of 0.1 cm^{-1} (Zhao *et al.* 2005). The SBF solution of soaking samples was refreshed every two days. After being soaked, the pellets were extracted from the solution rinsed with deionized water then dried in air at room temperature. The pellets without soaking in SBF are labelled as zero-day (0 d). The formation of an apatite layer on the surface of the pellets was investigated by X-Ray diffraction (XRD) for phase analysis, scanning electron microscopy (SEM) for morphology and energy dispersive spectroscopy (EDS) for elemental analysis.

Results and Discussion

Characterization of the bioactive glass powders

Bioactive glass powders were characterized by different analysis methods in order to evaluate the drying treatment and the influence of calcination temperature on the structure, morphology, and bioactivity of bioactive glass powders.

The phase formation behaviour of the bioactive glass powders derived from xerogel and aerogel at different calcination temperatures was investigated by XRD and the results patterns are shown in Fig. 1. The powders calcined at 400 °C and 600 °C for both xerogel and aerogel bioactive glass powders take an amorphous state indicating an intern disorder and glassy nature of these powders (Saboori *et al.* 2009; Radev *et al.* 2012). The heat treatment at 600 ºC resulted in some crystallite growth. While, the powders calcined at 800 °C illustrated a crystalline structure referred to the wollastonite ($CaSiO_3$) (Rainer *et al.* 2008),

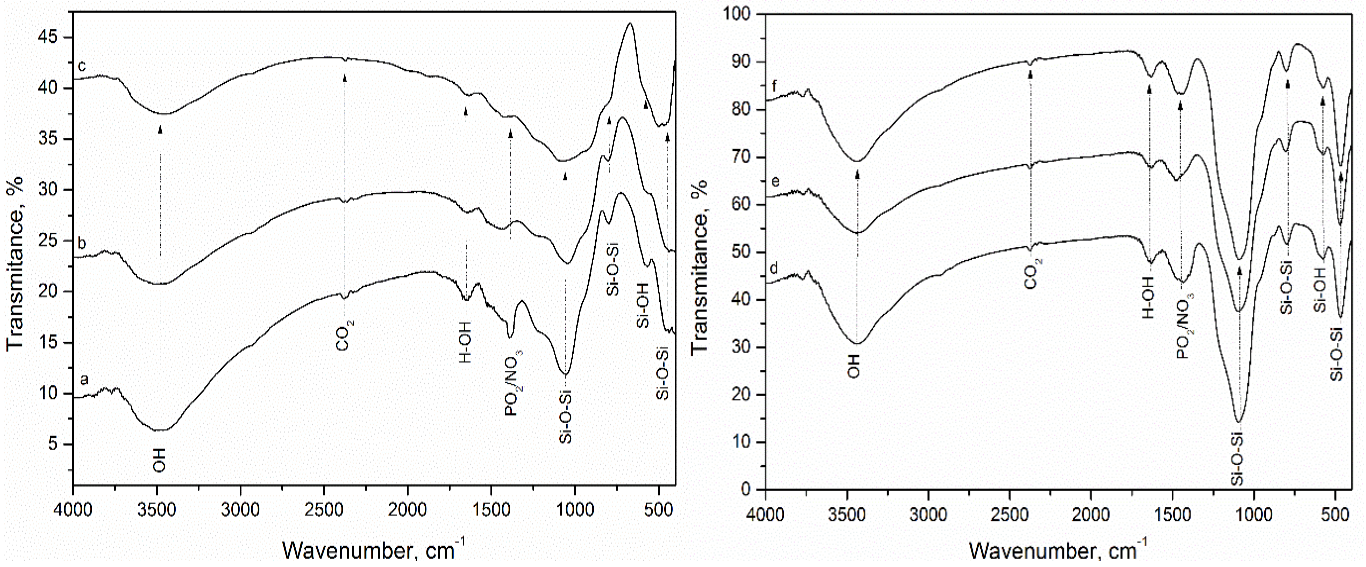

Fig. 2. FTIR spectra of bioactive glass powders: a– XG 400, b– XG 600, c– XG 800, d– AG 400, e– AG 600 and f– AG 800.

this specified that the crystallization process depending on the heat treatment conditions (Elbatal *et al.* 2003).

The formation of bioactive glass powders was further confirmed by FTIR spectral analysis illustrated in Fig. 2. All the samples showed an adsorption band at 1,036–1,082 cm^{-1} assigned to the Si-O-Si asymmetric bond stretching vibrations, the bond in the 785 – 790 cm^{-1} region is attributed to the symmetric Si-O-Si stretching vibrations (Lucas-Girot *et al.* 2011; Jiang *et al.* 2011) and the absorption around 453 – 463 cm^{-1} is due to the vibrational mode of the bending of Si-O-Si (Ma *et al.* 2011) indicating that all the samples are essentially composed of Si-O-Si network. These bands are narrower in the case of aerogel bioactive glass, and become larger with the increase of calcination temperature especially for xerogel

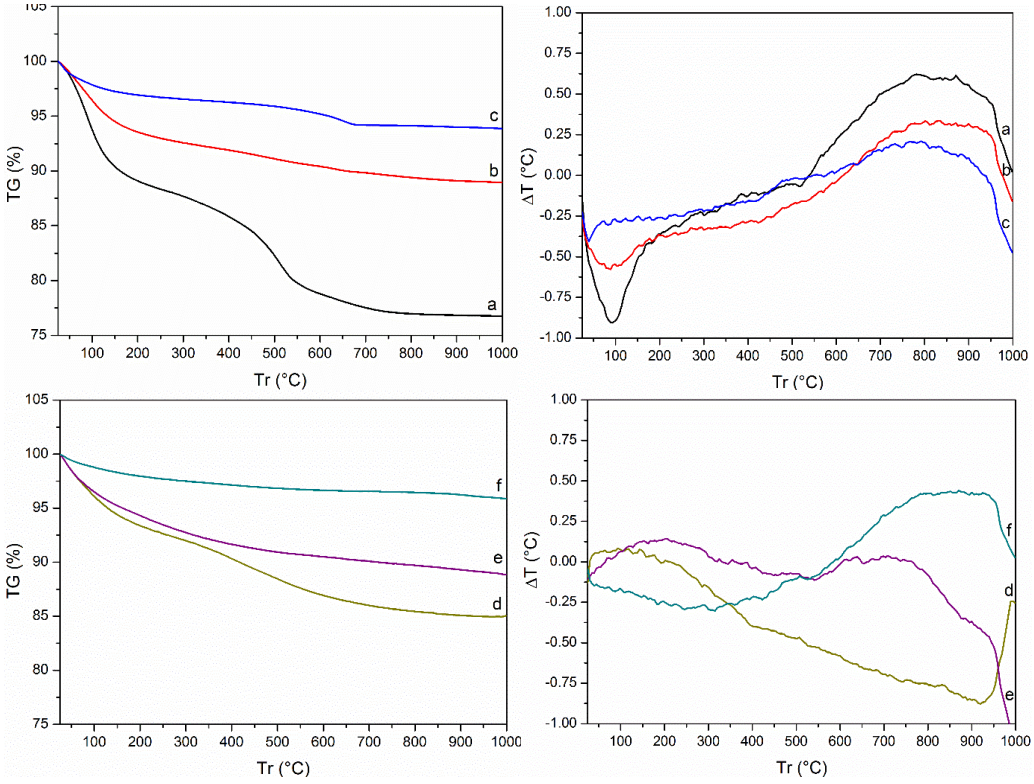

Fig. 3. TG/ DTA curves of prepared bioactive glass powders: a– XG 400, b– XG 600, c– XG 800, d– AG 400, e– AG 600 and f– AG 800.

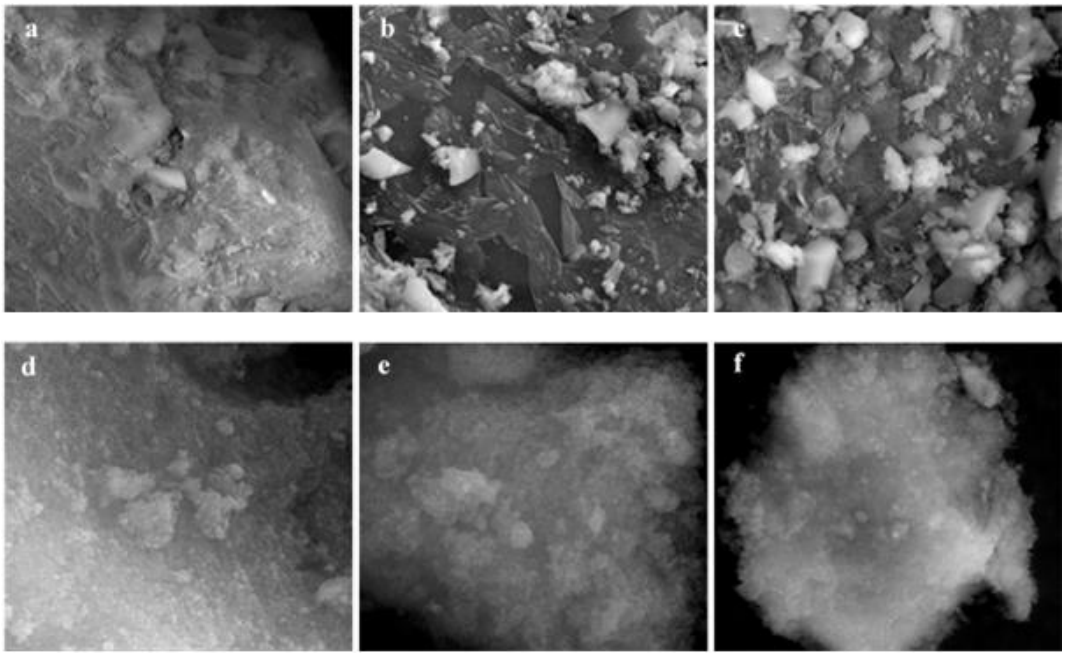

Fig. 4. SEM micrographs of bioactive glass powders: a– XG 400, b– XG 600, c– XG 800, d– AG 400, e– AG 600 and f– AG 800.

bioactive glass.

FTIR spectra involve the band around 956 cm^{-1} attributed to the stretching vibrations of Si-OH bonds (Tarasyuk *et al.* 2006), the band at 1,396 cm^{-1} is assigned to the vibrations of PO_2 and/or NO_3 groups (Qian *et al.* 2009), this band disappear in xerogel bioactive glass powders calcined at 600 °C and 800 °C but remains in the aerogel bioactive glass powders which can be explained by the transformation of PO_2 to the oxide P_2O_5 and/or the degradation of the nitrate NO_3 after calcination up to 600 °C in the case of the xerogel bioactive powder However, the remaining of the band at 1,396 cm^{-1} in the aerogel bioactive glass powders can be explained by their porous structure that contains small pores with a nanometric scale, which may imprison the PO_2 and/or NO_3 that are not reacted during the sol-gel process. The band at 2,372 cm^{-1} is attributed to the adsorption of CO_2 by the atmospheric (Hajiali *et al.* 2010). The weak inflection at 1,620 – 1,653 cm^{-1} and the broad band centred at 3,438 – 3,455 cm^{-1} are assigned to O–H band of adsorbed water and structural hydroxyl group respectively (Mehdipour and Afshar 2012). The samples were characterized by thermo-gravimetric and differential thermal analysis (TG/DTA). The Fig. 3 a-f shows TG/DTA traces of the developed bioactive glass powders. The results indicated that the weight loss decreases with increasing calcination temperature. Overall,

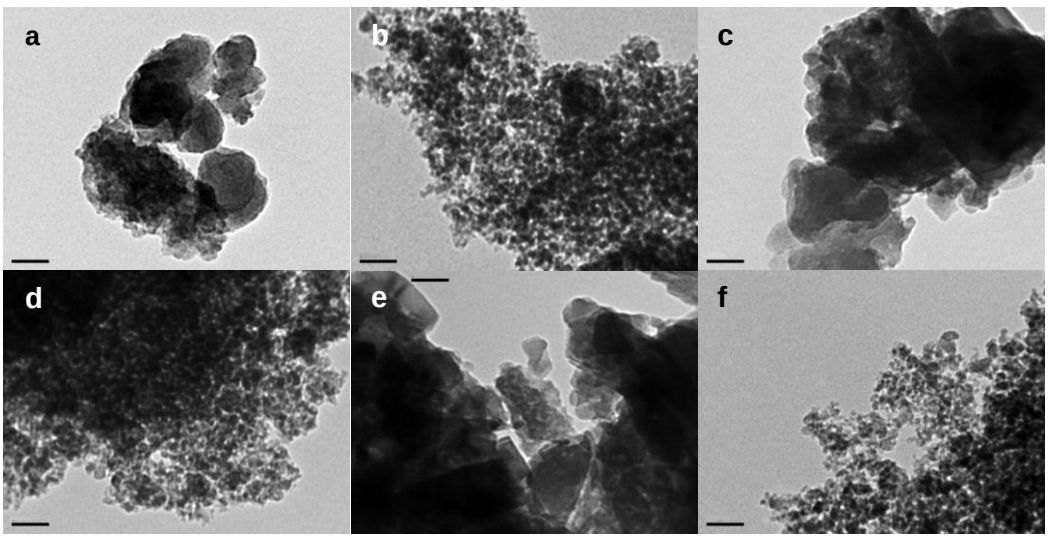

Fig. 5. TEM micrographs of prepared bioactive glass powders: a– XG 400, b– XG 600, c– XG 800, d– AG 400, e– AG 600 and f– AG 800.

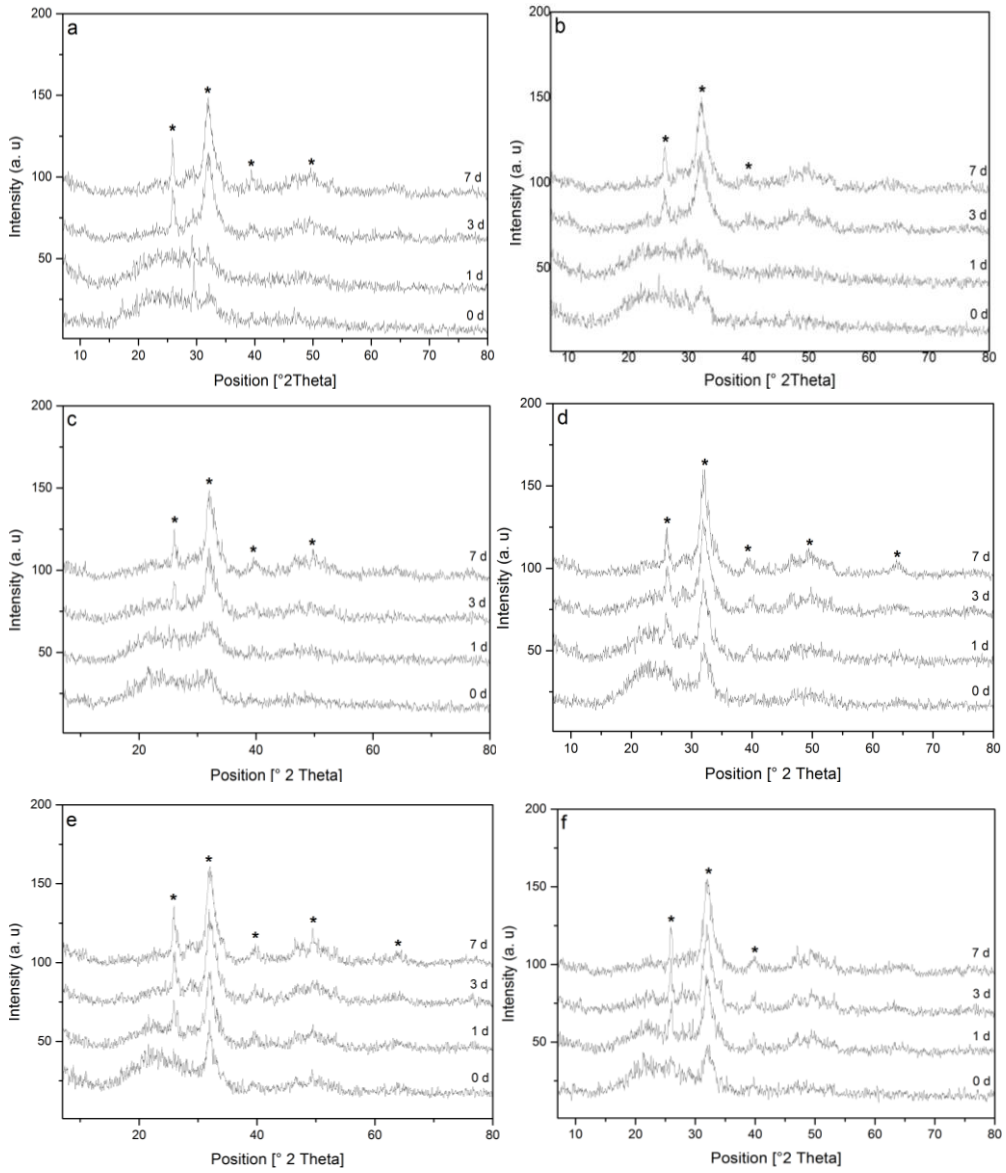

Fig. 6. XRD pattern of bioglasses before and after soaking in SBF solution for 1, 3 and 7 days:
a– XG 400, b– XG 600, c– XG 800, d– AG 400, e– AG 600 and f– AG 800.

xerogel bioactive glass powder calcined at 400 °C exhibits a greater weight loss with 23 % following by aerogel bioactive glass powder calcined at 400 °C with 15 %. The xerogel and aerogel bioactive glass powders calcined at 600 °C shows the same weight loss with 11 %. Whereas, the xerogel bioactive glass powder calcined at 800 °C shows a slight difference comparing to aerogel bioactive glass powder calcined at 800 °C with 6 % and 4 %, respectively.

The first mass loss stage occurs around 100 °C to 150 °C can be associated with the endothermic evaporation of the adsorbed water on the surface of the bioactive glass powders. A second weight loss occurs at 350 °C to 420 °C is due to the elimination of the remaining organic groups and the residual nitrates used during the sol-gel process (Riti *et al.* 2015). In addition, a third weight loss in the range of 550 °C to 660 °C is probably attributed to the polycondensation of residuals alkoxides (Cestari 2016), these loss weights can be explained by the glass transition temperature of bioactive glass particles (Gönen *et al.* 2016). A fourth weight loss at 690 °C and 850 °C is observed in the case of xerogel and aerogel bioactive glass powders calcined at 800 °C respectively can be attributed also to the structural transformation (Charoensuk *et al.* 2013). The different temperature of the fourth weight loss for the xerogel and aerogel bioactive glass powders could be attributed to their different particle size after the processes. The exothermic final process

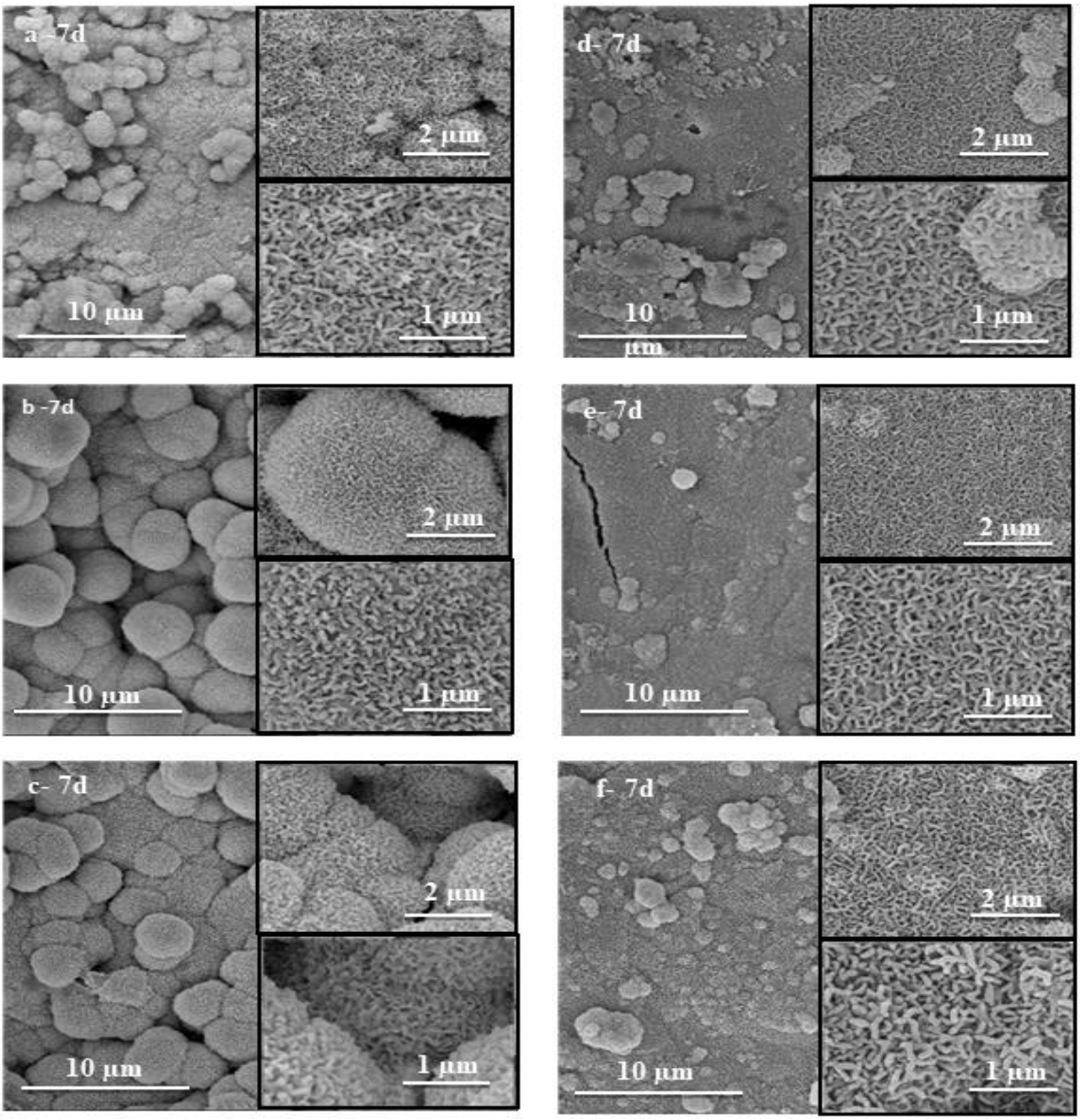

Fig. 7. SEM morphologies of bioactive glass pellets after soaking in SBF solution for 7 days: a– XG 400, b– XG 600, c– XG 800, d– AG 400, e– AG 600 and f– AG 800.

occurs at approximately 850 ºC and is related to the onset of crystallization. Thermal processing drives off the –OH groups, causing further formation of O–Si–O bonds. The nitrates were also removed during stabilization by thermal processing.

The drying conditions have an important effect on the porosity. SEM micrographs (Fig. 4) show that the obtained aerogel bioactive glass powders are less dense and more porous in comparison to xerogel bioactive glass powders. Aerogels are mostly constituted of agglomerate spherical particles with a spongy structure. Whereas xerogel bioactive glass powders are constituted of blocks, the apparition of white particles on the surface can be assigned to a crystal phase.

The values of particle size obtained from the results of image analysis of TEM micrographs also confirmed the SEM results. Xerogel bioactive glass powders are composed of uniform particles readily identified by TEM (Fig. 5 a-c).

The micrographs show a size particle between 20 nm to 100 nm with inhomogeneity of forms and

shapes. On the contrary, the aerogel network can be described as an assembly of clusters. These are formed by the aggregation of small homogeneous spherical particles with a size less than 10 nm. The TEM micrographs revealed that size of the bioactive glass powders increases with increasing of calcination temperature. This is can be explained by the structural contraction and densification during the sol-gel process of the developed bioactive glass powders and weight loss because of the polycondensation of the residual alkoxide (Cestari 2016).

In vitro assays

The Fig. 6 shows the XRD patterns of bioactive glass pellets prepared from xerogel and aerogel before and after soaking in SBF solution for 1, 3 and 7 days. It can be seen (Fig. 6), the apparition of two diffraction peaks at 26 and 32 ° (2θ) corresponding to (002) and (211) reflections of an apatite phase (Nayak *et al.* 2010; Ma *et al.* 2011). These peaks are observed after one day in the case of aerogel bioactive glass pellets (Fig. 6 d-f) and after 3 days for xerogel bioactive glass pellets (Fig. 6 a-c). These results indicate that an apatite crystal was deposited on the surface of the pallets. However, the diffraction peaks are less defined in xerogel bioactive glass pellets that may be due to a lower thickness of the calcium phosphate layer. The Elemental analysis of bioactive glass pellets before and after soaking in SBF for 1, 3 and 7 days was confirmed by energy dispersive X-ray analysis (EDS) technique. The results (Table 1) showed a remarkable increase in the intensity of calcium and phosphorus elements and reduction of the silica in all the pellets from the first day of immersion in SBF solution. The decrease of silica in xerogel and aerogel bioactive glass pellets calcined at 400 °C and 800 °C after 1 day of immersion showed a slight difference compared to bioactive glass pellets without immersion 0 day. After 7 days of immersion, we noticed the almost total disappearance of element Si and the appearance only of elements Ca and P which improve that the surfaces of the pallets are covered by an apatite layer. Excellent bioactive and resorbent properties of xerogel 63S bioactive glasses have been previously reported.

Table 1. The quantitative EDS analysis spectrum of bioglasses before and after soaking in SBF solution for 1, 3 and 7 days.

Samples /At [%]	C	O	Si	P	Ca
XG 400	5.74	61.01	21.04	2.68	9.52
XG 400, 1d	5.05	60.91	14.04	7.23	12.76
XG 400, 3d	7.43	57.26	0.47	12.07	22.76
XG 400, 7d	6.10	55.87	0.46	13.11	24.43
XG 600	8.67	58.59	20.20	2.61	9.93
XG 600, 1d	5.90	61.71	6.65	10.00	15.74
XG 600, 3d	5.53	57.71	0.89	12.17	23.70
XG 600, 7d	5.76	58.64	0.57	12.66	22.36
XG 800	5.41	58.12	23.52	2.94	10.02
XG 800, 1d	15.62	50.50	12.20	7.76	13.93
XG 800, 3d	14.61	50.55	4.66	10.68	19.51
XG 800, 7d	11.92	53.03	2.18	12.39	20.48
AG 400	3.99	60.98	23.76	4.11	7.16
AG 400, 1d	5.62	59.00	17.64	6.80	10.94
AG 400, 3d	9.18	57.08	4.72	11.21	17.82
AG 400,7d	8.11	58.25	1.53	12.45	19.66
AG 600	4.23	59.48	24.96	4.08	7.24
AG 600, 1d	12.91	52.63	7.57	10.69	16.20
AG 600, 3d	10.99	55.39	1.74	13.02	18.88
AG 600, 7d	16.09	51.83	1.10	12.61	18.37
AG 800	5.09	59.66	24.10	3.16	8.00
AG 800, 1d	5.36	57.43	14.57	8.75	13.89
AG 800, 3d	5.99	56.99	6.91	11.63	18.49
AG 800, 7d	6.00	56.74	2.84	12.70	21.72

The formation of bone-like apatite layer during bioactivity experiments was also evaluated by examining the change of surface morphology during the incubation in SBF solution. The Fig. 7 showed the surface morphology of samples before and after soaking in SBF for 1, 3 and 7 days. The results showed that the surface morphology changed with incubation periods. After 1 day soaking in SBF compared to 0 days as control, the micrographs revealed the formation of individual spherical apatite grain in the case of xerogel bioactive glass pellets and a fully covered surface with an extensive calcium phosphate precipitate with tiny flak on the shape for aerogel bioactive glass pellets. With increasing incubation periods, the formation of apatite grains increase too, after 3 days soaking the surface of xerogel bioactive glass pellets was fully covered by an apatite layer, and this layer was composed of numerous spherical particles. On the other hand, the more growing of the apatite layer for aerogel bioactive glass pellets. However, the density of the precipitate (apatite layer) increased significantly after 7 days of immersion. The ability of aerogel bioactive glass to promote rapid formation of apatite layer after only one day of soaking can be explained by faster

interchange between Ca^{2+} ions of aerogel bioactive glass and the H_3O^+ from SBF that can give rise to the formation of Si–OH groups on the surface of the pellets that induces the apatite nucleation (Petil *et al.* 2011). In addition, the rate of apatite formation depends on differences in the texture and morphology of xerogel and aerogel bioactive glass that improve the apatite deposition in SBF is extensive in rougher regions and sparse in flatter regions (Pereira *et al.* 1995; Petil *et al.* 2011). The formation of an apatite layer on the surface of the pellets is also more important when the temperature is increased. It found that the aerogel bioactive glass powder has a nanoparticle size and the formation of an apatite layer on the surface is faster and it is designated to compensate an organ or tissue deficient in a pathology, trauma or aging tissues (El-Kady *et al.* 2010; Hajiali *et al.* 2010).

Conclusions

In this study, ternary bioactive glass powders were successfully synthesized via the sol-gel route from two types of dried gel: xerogel and aerogel. The results obtained show that the texture of elaborated bioactive glass powders is strongly influenced by the drying conditions of the gels and the calcination temperature. It found that the aerogel bioactive glass powders are characterized by less dense and spongy structure with a particles size less than 10 nm and an apatite layer is obtained after only one day of immersion in SBF solution. However, the xerogel bioactive glass powders presented a dense structure with a particle size around 100 nm and a surface covered with an apatite layer after three days of immersion in SBF solution. The bioactive glass powders calcined at 800 °C presented a good properties and *in vivo* tests will be interesting for this powder in order to improve its viability to be used in regenerative medicine: filling bone defects, prosthetic coatings in orthopedic surgery, maxillofacial and dental.

References

Al-Noaman A, Rawlinson SCF, Hill RG (2012) The role of MgO on thermal properties, structure and bioactivity of bioactive glass coating for dental implants. J. Non-Cryst. Solids 358: 3019-3027.

Bellucci D, Cannillo V, Sola A (2011) Calcium and potassium addition to facilitate the sintering of bioactive glasses. Mater. Lett. 65: 1825-1827.

Catauro M, Bollino F, Renella RA, Papale F (2015) Sol gel synthesis of glasses: influence of the heat treatment on their bioactivity and biocompatibility. Ceram. Int. 41: 12578-12588.

Cestari A (2016) Sol-gel methods for synthesis of aluminosilicates for dental applications. J. Dentistry 55: 105-113.

Charoensuk T, Sirisathitkul Ch, Boonyang U (2013) Thermal analysis of mesoporous and macroporous bioactive glasses synthezed by Sol-Gel method. Rev. Rom. Mater. 43: 320-325.

Deligianni DD, Katsala ND, Koutsoukos PG, Missirlis YF (2001) Effect of surface roughness of hydroxyapatite on human bone marrow cell adhesion, proliferation, differentiation and detachment strength. Biomaterials 22: 87-96.

Doostmohamadi A, Monshi A, Fathi MH, Karbasi S, Braissant O, Daniels QU (2011) Direct cytotoxicity evaluation of 63S bioactive glass and bone-derived hydroxyapatite particles using yeast model and human chondrocyte cells by microcalorimetry. J. Mater. Sci. Mater. Med. 22: 2293-2300.

ElBatal HA, Azooz MA, Khalil EMA, Soltan Monem A, Hamdy YM (2003) Characterization of some bioglass-ceramics. Mater. Chem. Phys. 80: 599-609.

El-Kady AM, Saad EA, El-Hady ABM, Farag MM (2010) Synthesis of silicate glass/poly (L-lactide) composite scaffolds by freeze-extraction technique: Characterization and *in vitro* bioactivity evaluation. Ceram. Int. 36: 995-1009.

Erol-Taygun M, Zheng K, Boccaccini AR (2013) Nanoscale Bioactive Glasses in Medical Applications. Int. J. Appl. Glass Sci. 4: 136-148.

Gönen SÖ, Erol TM, Aktürk A, Küçükbayrak S (2016) Fabrication of nanocomposite mat through incorporating bioactive glass particles into gelatin/poly(ε-caprolactone) nanofibers by using Box-Behnken design. Mater. Sci. Eng. C 67: 684-693.

Hajiali H, Karbasi S, Hosseinalipour M, Rezaie HR (2010) Preparation of a novel biodegradable nanocomposite scaffold based on poly (3-hydroxybutyrate)/bioglass nanoparticles for bone tissue engineering. J. Mater. Sci. Mater Med. 21: 2125-2132.

Jiang P, Lin H, Xing R, Jiang J, Qu F (2011) Synthesis of multifunctional macroporous-mesoporous TiO_2-bioglasses for bone tissue engineering. J. Sol-Gel Sci. Technol. 61: 421-428.

Kokubo T (1990) Surface chemistry of bioactive glass-ceramics. J. Non-Cryst. Solids 120: 138-151.

Leonor IB, Sousa RA, Cunha AM, Reis RL (2002) Novel starch thermoplastic/Bioglass composites: Mechanical properties, degradation behavior and in-vitro bioactivity. J. Metr. Sci. Mater. Med. 13: 939-945.

Li HC, Wang DG, Hu JH, Che CZ (2013) Effect of various additives on microstructure, mechanical properties, and *in vitro* bioactivity of sodium oxide-calcium oxide-silica-phosphorus pentoxide glass-ceramics. J. Colloid

Interface Sci. 405: 296-304.
Lucas-Girot A, Mezahi FZ, Mami M, Oudadesse H (2011) Abdelhamid Harabi. Marie Le Floch. Sol–gel synthesis of a new composition of bioactive glass in the quaternary system SiO_2-CaO-Na_2O-P_2O_5 Comparison with melting method. J. Non-Cryst. Solids 357: 3322-3327.
Ma J, Chen CZ, Wang DG, Hu JH (2011) Synthesis, characterization and *in vitro* bioactivity of magnesium-doped sol-gel glass and glass-ceramics. Ceram. Int. 37: 1637-1644.
Mehdipour M, Afshar A (2012) A study of the electrophoretic deposition of bioactive glass-chitosan composite coating. Ceram. Int. 38: 471-476.
Nayak JP, Kumar S, Bera J (2010) Sol-gel synthesis of bioglass-ceramics using rice husk ash as a source for silica and its characterization. J. Non-Cryst. Solids 356: 1447-1451.
Pereira MM, Clark AE, Hench LL (1995) Effect of texture on the rate of hydroxyapatite formation on gel-silica surface. J. Am. Ceram. Soc. 78: 463-468.
Petil O, Zanotto ED, Hench LL (2011) Highly bioactive P_2O_5- Na_2O- CaO-SiO_2 glass-ceramics. J. Non-Cryst. Solids. 292: 115-126.
Qian J, Kang Y, Wei Z, Zhang W (2009) Fabrication and characterization of biomorphic 45S5 bioglass scaffold from sugarcane. Mater. Sci. Eng. C 29: 1361-1364.
Radev L, Hristova K, Jordanov V, Fernandes MHV, Salvado IMM (2012) *In vitro* bioactivity of 70 Wt.% SiO_2- 30 Wt.% CaO sol-gel glass, doped with 1,3 and 5 Wt.% NbF_5. Centr. Eur. J. Chem. 10: 137-145.
Rainer A, Giannitelli SM, Abbruzzese F, Traversa F, Licoccia S, Trombetta M (2008) Fabrication of bioactive glass-ceramic foams mimicking human bone portions for regenerative medicine. Acta Biomater. 4: 362-369.
Riti PI, Vulpoi A, Simon V (2015) Effect of pH dependent gelation time and calcination temperature on silica network in SiO_2-CaO and SiO_2-MgO glasses. J. Non-Cryst. Solids. 411: 76-84.
Saboori A, Rabiee M, Moztarzadeh F, Sheikhi M, Tahriri M, Karimi M (2009) Synthesis, characterization and *in vitro* bioactivity of sol-gel-derived SiO_2-CaO-P_2O_5-MgO bioglass. Mater. Sci. Eng. C 29: 335-340.
Tarasyuk E, Shilova OA, Bochkin AM, Pomogailo AD (2006) Investigation into the influence of organic modifiers and ultradispersed hybrid fillers on the structure and properties of glass-ceramic coating prepared by the sol-gel method. Glass Phys. Chem. 32: 439-447.
Valerio P, Pereira MM, Goes AM, Leite MF (2004) The effect of ionic products from bioactive glass dissolution on osteoblast proliferation and collagen production. Biomaterials 25: 2941-2948.
Zhao W, Wang J, Zhai W, Wang Z, Chang J (2005) The self-setting properties and *in vitro* bioactivity of tricalcium silicate. Biomaterials 26: 6113-6121.
Zhitomirsky D, Roether JA, Boccaccini AR, Zhitomirsky I (2009) Electrophorotic deposition of bioactive glass/polymer composite coating with and without HA nanoparticle inclusions for biomedical applications. J. Mater. Process. Technol. 209: 1853-1860.